Icarus 199 (2009) 442–448

Contents lists available at ScienceDirect

Icarus

www.elsevier.com/locate/icarus

Rain and dewdrops on titan based on in situ imaging

Erich Karkoschka *, Martin G. Tomasko

Lunar and Planetary Laboratory, University of Arizona, Tucson, AZ 85721-0092, USA

ARTICLE INFO

Article history:
Received 2 July 2008
Revised 17 September 2008
Accepted 28 September 2008
Available online 17 November 2008

Keywords:
Titan

ABSTRACT

The Descent Imager/Spectral Radiometer (DISR) of the Huygens probe was in an excellent position to view aspects of rain as it descended through Titan's atmosphere. Rain may play an important part of the methane cycle on Titan, similar to the water cycle on Earth, but rain has only been indirectly inferred in previous studies. DISR detected two dark atmospheric layers at 11 and 21 km altitude, which can be explained by a local increase in aerosol size by about 5–10%. These size variations are far smaller than those in rain clouds, where droplets grow some 1000-fold. No image revealed a rainbow, which implies that the optical depth of raindrops was less than ~0.0002/km. This upper limit excludes rain and constrains drizzle to extremely small rates of less than 0.0001 mm/h. However, a constant drizzle of that rate over several years would clear the troposphere of aerosols faster than it can be replenished by stratospheric aerosols. Hence, either the average yearly drizzle rate near the equator was even less (<0.1 mm/yr), or the observed aerosols came from somewhere else. The implied dry environment is consistent with ground-based imaging showing a lack of low-latitude clouds during the years before the Huygens descent. Features imaged on Titan's surface after landing, which might be interpreted as raindrop splashes, were not real, except for one case. This feature was a dewdrop falling from the outermost baffle of the DISR instrument. It can be explained by warm, methane-moist air rising along the bottom of the probe and condensing onto the cold baffle.

1. Introduction

After methane was discovered in Titan's atmosphere, it became clear that it is not stable in the upper stratosphere and must be replenished from the surface by evaporation from a global ocean, by large areas of lakes, or other mechanisms (Lunine et al., 1983). This caused speculation of an active methane cycle on Titan, possibly similar to the water cycle on Earth. Observational evidence followed. Evidence of tropospheric clouds came from spectroscopy (Griffith et al., 1983) and imaging with near-infrared adaptive optics (Brown et al., 2002; Roe et al., 2002), in particular near Titan's South Pole. Cassini monitored the evolution of cloud activity near the South Pole on a time scale of one hour during its first fly-by (Porco et al., 2005). Fainter clouds were observed near 40° southern latitude (Roe et al., 2005). DISR revealed channels indicative of past fluvial activity (Tomasko et al., 2005). The Cassini Radar recorded many more channels at other locations (Elachi et al., 2005) and found strong evidence for large lakes near Titan's North Pole (Stofan et al., 2007).

Theoretical investigations indicated various possibilities of methane rain, from violent thunderstorm-like activity (Hueso and Sánchez-Lavega, 2006) to general, light drizzle (Tokano et al., 2006). This encouraged observers to look for more hints of rain and drizzle. Dark areas on Titan's morning side were found by near-infrared imaging probing the lower atmosphere, and interpreted as drizzle (Ádámkovics et al., 2007), although these features could also be due to an imperfect accounting for imaged surface features on Titan (Kim et al., 2008).

In this investigation, we focus on the subtle features visible in DISR images, which may give clues about rain or drizzle during and before the descent of Huygens onto Titan's surface on January 14, 2005. Various aspects connected to rain on Titan are discussed in separate sections: a search for rain cloud layers to detect the creation of rain (Section 2), a search for rainbows to monitor falling rain (Section 3), a search for the effects of past rain (Section 4), a search for surface splashes of rain (Section 5), and a search for imaging of individual drops (Section 6).

2. Rain clouds

On Earth, rain is associated with optically thick clouds of growing water drops. Similar clouds layers would have been easily detectable by the Side Looking Imager (SLI) of the Descent Imager/Spectral Radiometer (DISR) onboard the Huygens spacecraft as it descended onto Titan, if they were present during the descent. However, it is conceivable that clouds for rain or drizzle on Titan are much more subtle.

* Corresponding author. Fax: +1 520 621 4933.
E-mail address: erich@lpl.arizona.edu (E. Karkoschka).

0019-1035/$ – see front matter
doi:10.1016/j.icarus.2008.09.020

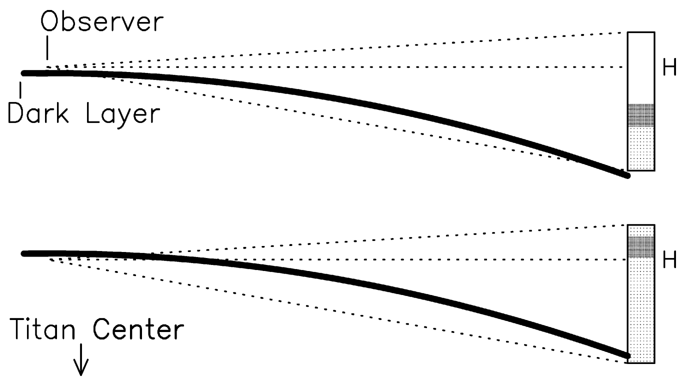

Fig. 1. Expected location of the image of a dark layer for an observer slightly above the layer (top) and slightly below (bottom). In the first case, the layer is visible looking down, below the horizontal direction "H" (rectangle at right). In the second case, it is best visible looking slightly up.

The SLI looked at a 25° wide and 50° high field of view, covering the zenith angles 85–135°, although these limits varied by a few degrees as Huygens tilted back and fourth. The signal-to-noise ratio was kept near 200 throughout the descent by adjusting exposure times. For the detection of horizontal layers, this ratio could be improved by another factor of 11 through averaging of the 128 horizontal pixels of the SLI. In reality, however, all features with less than about 0.2% contrast were lost by data compression, limiting the signal-to-noise ratio to about 500. This still made the SLI a very sensitive instrument for detecting large features of low contrast, such as horizontal layers, rainbows, or halos.

An early investigation of the SLI images yielded only one candidate for a cloud layer, a dark layer at 21 km altitude (Tomasko et al., 2005). The layer was about 1 km thick, and its absorption optical depth was 0.001. We scrutinized all SLI images taken during the descent to obtain a more complete characterization of subtle layers. Subtle layers are only detectable if the observer is near the altitude of the layer. If the observer is slightly above or below a layer, it is best detectable looking below or above the horizontal direction, respectively (Fig. 1 top and bottom, respectively).

The dark layer at 21 km had a contrast too low to be visible with the naked eye or on SLI images without a contrast stretch. The general, vertical brightness gradient was much stronger than the 1–2% brightness variation due to the dark layer. In order to increase the visibility of such layers, we removed the general brightness gradient for all SLI images in the following way.

We selected the area between 88 and 96° zenith angle (from 2° above the horizontal to 6° below), based on published geometric data (Table 1 of Karkoschka et al., 2007). We fitted the data numbers to a seven-parameter function. Six terms are the polynomials up to combined order two in the horizontal and vertical direction, respectively. The seventh term is a cubic function in the vertical direction. After removal of these smooth functions, the remaining features are displayed in Fig. 2 with the contrast enhanced 50-fold. Altitudes and average scattering angles are listed for each image.

Even with such extreme contrast enhancement, most of the images of Fig. 2 are featureless. The surface became detectable at the bottom of the displayed area (6° below horizontal) around 10 km altitude. The horizon became detectable near 3 km altitude, and it got sharper as Huygens approached the surface. After landing, the horizon was elevated by more than 1° due to nearby hills. Although the surface was only slightly darker than the sky, it appears black in Fig. 2 due to the 50-fold contrast enhancement.

The dark layer at 21 km is obvious in the images taken at 20.6–20.8 km altitude. The images at 22–23 km altitude show a hint of the dark layer below the horizontal. At lower altitudes of 20.0–20.2 km, in particular in the 20.1-km image, the layer is detectable looking slightly up. The dark layer was centered somewhere between 20.5 and 21.0 km altitude.

In principle, the dark layer could be due to an absorbing gas. It could be due to darker aerosols. Since the aerosol optical depth was about 0.05/km, the estimated absorption optical depth of 0.001 with a 1-km thickness corresponds to a moderate decrease of the aerosol's single scattering albedo of 0.02.

With both explanations, the contrast of the layer should have been almost independent of the viewing direction, which is contradicted by the observations. Among the three images at 20.6–20.8 km altitude, the highest contrast was for the lowest scattering angle and vice versa. The same anti-correlation is observed for the images at 20.0–20.2 km altitude and those at 22.4–23.3 km altitude (cf. Fig. 2). This strongly suggests that the aerosols in the layer had a different phase function than the aerosols above and below.

We can speculate what change of aerosol parameters could cause a lower phase function at scattering angles of 60–120°. The best candidate is a larger aerosol size. Aerosols in the nominal model (Section 3 of Tomasko et al., 2008) are fractals with 3000 monomers. If we increase the number of monomers at 21 km altitude from 3000 to 4000, the model intensities decrease by 1.6, 1.3, and 0.9% for scattering angles of 57, 82, and 115°, while the observed values are 2, 2, and 1%, respectively. Thus, an increased aerosol volume by about 30%, corresponding to an increased aerosol effective radius of about 10%, can roughly explain the magnitude of the observed intensity drop and its variation with scattering angle. A best fit to the data at 21 km occurs for an increase of the aerosol radius of 13%, but neither our data accuracy nor the modeling technique allows us to give a second significant digit.

This result needs to be considered with respect to the general change of aerosol sizes with altitude. The aerosol radius may increase from 0.7 μm at 40 km altitude to 10 μm near the surface (Fig. 51 of Tomasko et al., 2008), which is an average increase of 7%/km. Adding the local variation at 21 km to this general trend, the aerosols at 21 km altitude were of similar size as those at 20 or 19 km, but significantly larger than those at 22 km altitude. Note that these considerations are only best guesses since aerosol sizes and shapes are not perfectly constrained by the data.

The other obvious dark layer in the data set is at 10.5–11 km altitude. It is best seen from two images taken at 10.9 km altitude. It was detectable down to 10.3 km altitude looking slightly up. There is also a hint for it from 12.1–12.4 km altitudes, looking slightly down. Just like the 21 km layer, the contrast of the dark layer is very dependent on scattering angle, and the dependence is in the same way in both layers. Thus, this layer may have an explanation very similar to that for the 21-km layer. In this case, the effective absorption optical depth is only half as much, about 0.0005, and the best guess for the irregularity of the aerosol size is on the order of 5%.

The data below 10 km altitude are less suitable for the detection of subtle layers, since the data compression focused on the accurate rendition of surface features, which reduced the sensitivity for subtle features in the sky. Furthermore, narrow features seen from lower altitudes close to the horizon produced a "ringing" effect next to the relatively sharp horizon with its high contrast. The best candidate for another dark layer comes from the image taken at 7.2 km altitude, but this layer is not seen in another image and is thus a questionable detection.

In summary, DISR monitored the growth of aerosols towards lower altitudes, recording irregularities of about 5–10% in aerosol size. If particles were growing to raindrops, their sizes would have increased some 1000-fold, from the order of a micrometer for aerosols to the order of a millimeter for raindrops. It is inconceivable that DISR missed a region of particle growth by a factor of